CARBON MOLECULAR SIEVE MEMBRANES FOR AGGRESSIVE SOUR GAS SEPARATIONS

A Thesis
Presented to
The Academic Faculty

By

Ruben Kyle Kemmerlin

In Partial Fulfillment
Of the Requirements for the Degree
Master of Science in Chemical Engineering

Georgia Institute of Technology

December, 2012

CARBON MOLECULAR SIEVE MEMBRANES FOR AGGRESSIVE SOUR GAS SEPARATIONS

Approved by:

Dr. William J. Koros, Advisor
School of Chemical & Biomolecular Engineering
Georgia Institute of Technology

Dr. Krista S. Walton
School of Chemical & Biomolecular Engineering
Georgia Institute of Technology

Dr. P. Jason Williams
Projects and Technology – Innovation,
Research, and Development
Shell Global Solutions (US) Inc.

Date Approved: August 8, 2012

This thesis is dedicated to those I love the most,
my parents.

ACKNOWLEDGEMENTS

TABLE OF CONTENTS

Page

LIST OF TABLES

LIST OF FIGURES

Page

SUMMARY

In this study the conditioning of CMS membranes with H_2S was studied for the determination of the acid gas steady state transport properties. It had been shown that the transport properties of CMS membranes varies as a function of H_2S exposure making the conditioning protocol an important step in identifying the steady state properties of CMS membranes. It was important to identify whether the conditioning seen during initial sour gas separations continued until the membrane was effectively "shut down" or if the conditioning would reach a steady state. The results of this study indicate that CMS membranes reach a conditioned steady state upon sufficient H_2S exposure.

The conditioned steady state has been shown to be the same state for both an extended conditioning protocol using high pressure mixed gas and a rapid conditioning protocol using pure H_2S. The rate of conditioning does vary between the two conditioning protocols as the rapid conditioning protocol takes 48 hours less to reach the conditioned steady state.

The results of this study also show that oxygen doping during the formation of the CMS membrane affects the final, conditioned steady state transport properties. The presence of oxygen at the size discriminating ultramicropores increases the degree of H_2S conditioning likely through the formation of surface sulfoxides. It has been shown with three separate oxygen doping concentrations that the conditioned steady states exhibit different transport properties, and there was a larger decrease in permeation as the amount of oxygen doping increased for the H_2S conditioned membranes.

CHAPTER 1

INTRODUCTION

1.1 Natural Gas Motivation

Carbon based non-renewable energy resources remain the dominant fuels in worldwide energy consumption. These energy resources are oil, coal, and natural gas, and the consumption of all energy resources is expected to increase over the next 30 years [1,2]. This expected increase is shown in Figure 1.1. Natural gas is the preferred fuel source for electricity production and industrial uses due to its lower carbon emissions and high combustion efficiency compared to oil and coal. The annual global consumption of natural gas exceeded 111 trillion cubic feet in 2008 and is expected to increase to over 169 trillion cubic feet by 2035 [1].
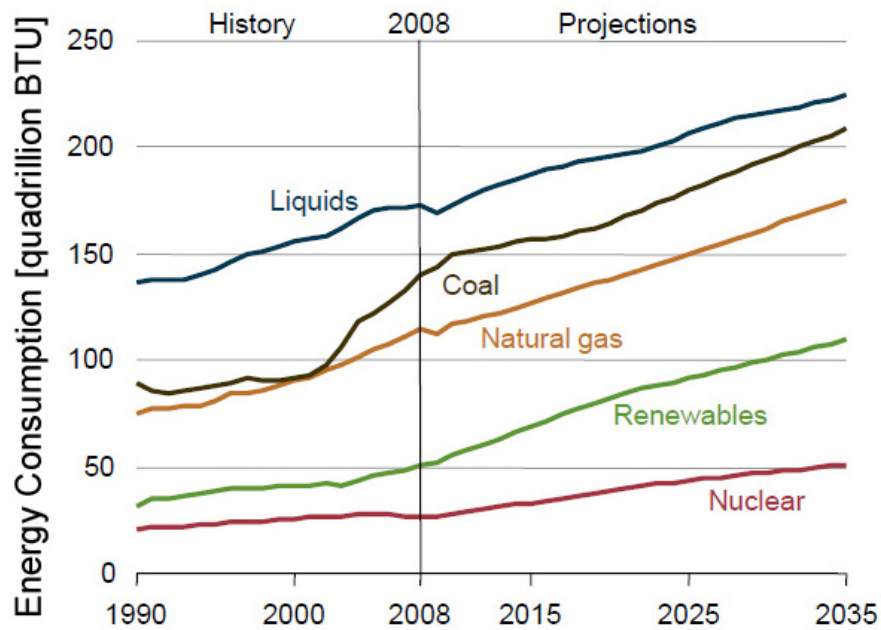
Figure 1.1: World energy production projections according to the US energy information administration[1]. Energy production from all sources is expected to increase significantly as world energy demand increases.

US consumption alone accounted for 24 trillion cubic feet in 2010 and is expected to increase to as much as 28 trillion cubic feet by 2035 [2]. With recent large findings of

shale natural gas resources within the US, there is an evident increase in natural gas production as shown in Figure 1.2. With this high expected demand it becomes important for industry experts to economically extract natural gas reservoirs and provide a safe product to end users.
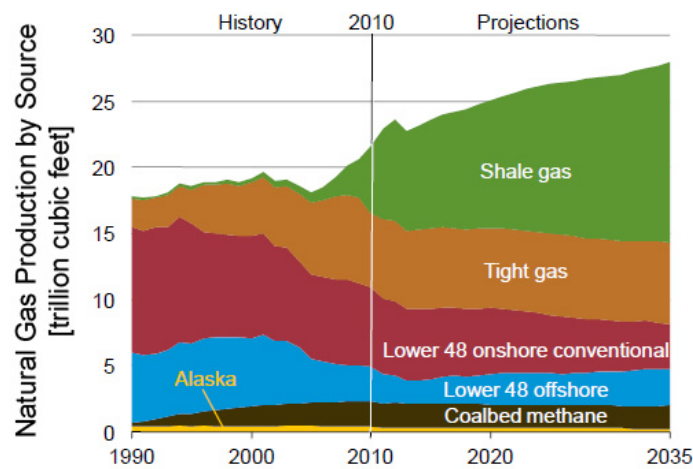
Figure 1.2: US natural gas production projections. The significant increase in expected production necessitates the best technology available be used for natural gas production.

There are challenges to natural gas recovery. Natural gas is predominantly methane with various levels of impurities. These impurities are typically water, carbon dioxide, hydrogen sulfide, heavier hydrocarbons (C2+), and inert gases (mostly nitrogen and small amounts of noble gases) [3,4]. These impurities should be removed in order to meet US pipeline specifications for producers to supply the natural gas network within the US. These pipeline specifications are shown in Table 1.1 along with typical US well compositions and how relatively abundant each well composition can be found.

1.2 Acid Gas Contaminants

The acid gas impurities of note are both carbon dioxide and hydrogen sulfide. Natural gas that contains hydrogen sulfide impurities greater than the pipeline specification is called sour gas. The process(es) used to remove these acid gas impurities are called sour gas sweetening. There are several significant reasons why it's

important to sweeten sour gas. From a processing standpoint, the sweetening of sour gas is very important because the acid gases present in sour gas can cause severe corrosion in both pipelines and processing equipment in the presence of water. All contaminants, both acid gases and inerts, dilute the natural gas and therefore increase both processing and transportation cost. Additionally, acid gases lower the overall heating value of the natural gas making it less valuable to electricity producers and industrial uses per unit volume.

Table 1.1: US Pipeline specification and typical well composition. Adapted from Baker et al. and Besso [3,4].

Component	Specification	U.S. Well Composition	% of Total U.S. Gas
Methane	-	75 – 90%	-
CO_2	< 2 %	< 1 %	72 %
		1 – 3 %	18 %
		3 – 10 %	7 %
		> 10 %	3 %
H_2O	< 120 ppm	800 – 1,200 ppm	-
H_2S	< 4 ppm	< 4 ppm	76 %
		4 – 1,000 ppm	11 %
		1,000 – 10,000 ppm	4 %
		> 10,000 ppm	8 %
C_{3+} Content	950 – 1,050 Btu/scf Dew Point: < -20 °C	-	-
Inert Gas (He, N_2)	< 4 %	> 4 %	14 %

This table was slightly modified from the original table.

1.3 Sour Gas Sweetening Technologies

There are several separation technologies that are commonly used for natural gas sweetening: absorption, adsorption, cryogenic distillation, and membrane processes. The most common separation process is absorption and most are typically amine absorption processes. Amine absorption separation units have severe limitations for many natural gas sweetening projects. Absorption towers must be very large and this size scales with the amount of acid gas that must be removed. Towers are therefore a costly capital expenditure. Absorption processes also have high costs associated with maintenance and waste disposal. Waste disposal is particularly significant because all

spent solvent or sorbent packing must be either disposed of or regenerated, both of which have their associated costs.

1.4 Membrane Technology

Membranes are an attractive alternative to absorption process due to their ability to withstand aggressive feed conditions and the high surface area to volume ratio in current hollow fiber membrane modules. The modular size of membrane units also lends itself to remote and offshore applications where other separation processes would be impractical [3]. Membranes also have the advantage of being both water and solvent free which saves on the capital cost of storing and the operating costs associated with maintenance and disposal of these liquids.

There exists a tradeoff between the permeability and permselectivity of various gas pairs with typical polymeric membranes [7]. Carbon molecular sieve (CMS) membranes have been shown to surpass this upper bound tradeoff which makes CMS membrane modules even more favorable for sour gas sweetening, see Figure 1.4. Similar to the previously mentioned amine absorption towers, the membrane surface area scales with the amount of sour gas that must be processed. In order to obtain large throughputs of natural gas the membrane modules require large membrane areas. Hollow fiber membranes have been developed to significantly increase the surface area to volume ratio compared to other membrane module configurations. Figure 1.3 illustrates some examples of membrane module configurations and their relative surface area to volume ratios. Therefore, the development of new membrane materials in a hollow fiber configuration also makes membrane separation units more attractive.
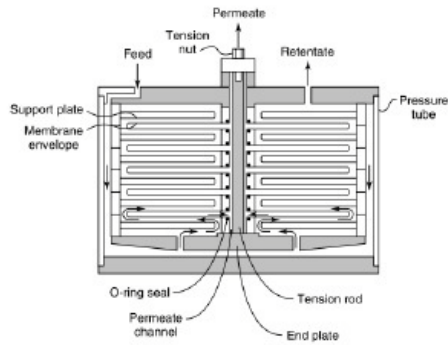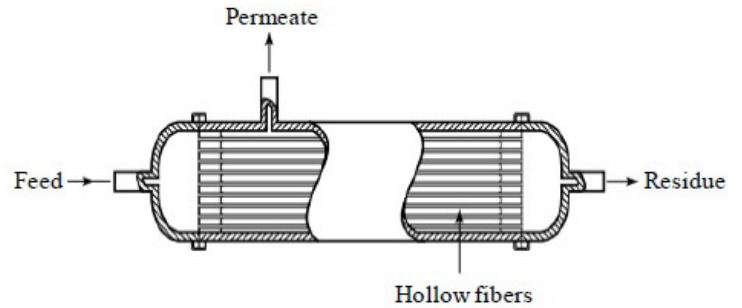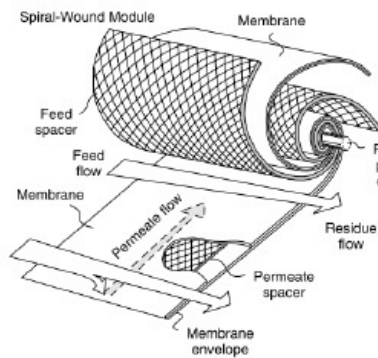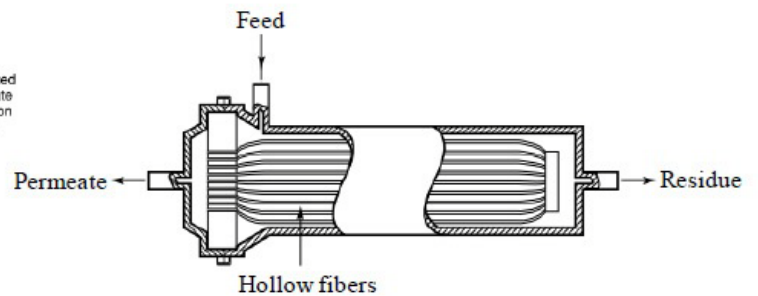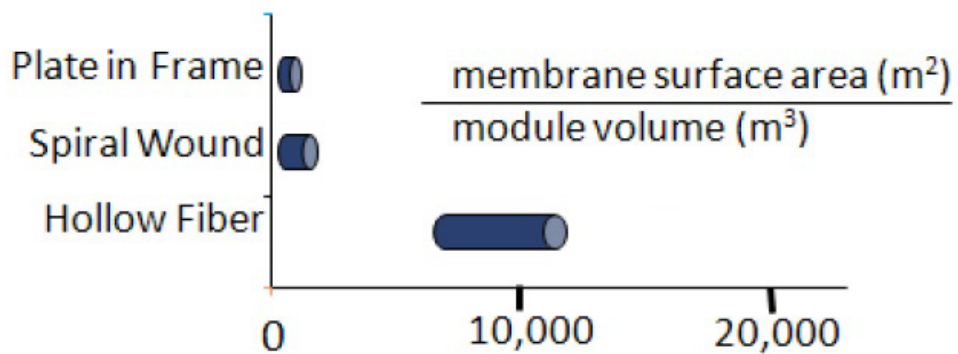
Figure 1.3: Common membrane configurations and their relative surface area to volume ratios, adapted from Kiyono [6].
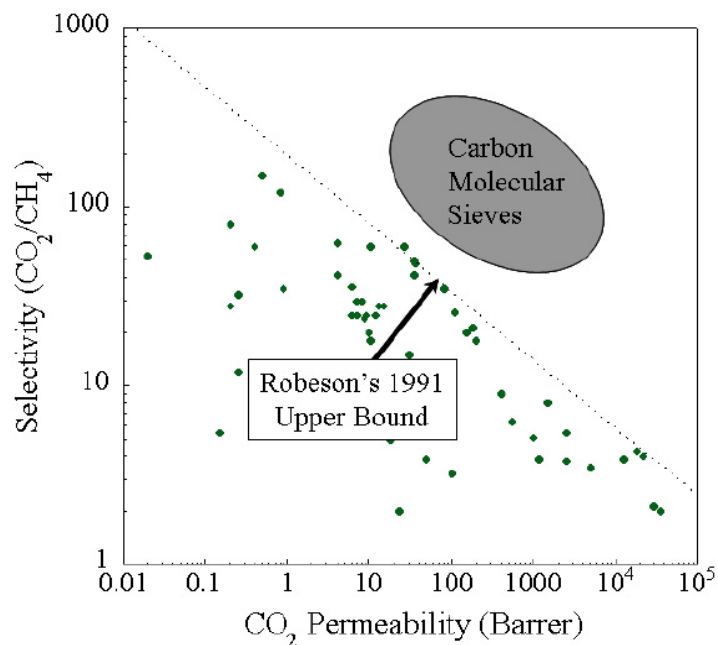
Figure 1.4: The Robeson plot with the upper bound identified for CO_2/CH_4 separations, adapted from [6]. Note that CMS membranes exceed the upper bound.

1.5 Research Objectives

As it has been shown, CMS membranes have favorable separation properties that make them viable alternatives to both polymeric membranes and other current technologies [6]. Recent research has shown that commercially attractive CMS membranes can be produced under inert pyrolysis atmosphere which allows for an easier scale-up to industrial production levels. Additionally, preliminary H_2S/CH_4 separation data showed attractive productivities and efficiencies. More importantly, researchers in the Koros Research Group noticed a significant change in permeability properties as the membranes were continually exposed to moderate levels of H_2S (10/90 H_2S/CH_4 feed at 50 psia at 35 °C) [6]. This change in permeability properties is being referred to as H_2S conditioning.

The hypothesis tested in this research project is that the separation properties, both the pure gas permeabilities and the ideal selectivities, will approach steady state values at a rate that are based on the time exposed to the same chemical activity of H_2S.

6

In order to test this hypothesis, two separate H_2S conditioning protocols were proposed. The first conditioning protocol tested is being referred to as extended conditioning. Extended conditioning involves exposing the CMS hollow fiber module to high pressure (1135 psia) mixed gas, (20.0 mol % H_2S, 20.0 mol % CO_2, 60.0 mol % CH_4). This mixed gas feed composition and pressure models some of the most aggressive natural gas deposits in the world. The idea behind extended conditioning is to see how the membrane separation properties would change in a highly aggressive industrial application. The second conditioning protocol is referred to as rapid conditioning. Rapid conditioning involved exposing the CMS hollow fiber module to high pressure (150 psia) pure H_2S. This rapid conditioning was proposed as way to rapidly stabilize CMS membranes under the most demanding conditions. The rapid conditioning approach was designed to determine whether or not the CMS membranes approach the same steady state as the extended conditioning alternative. The rapid conditioning approach would be more favored for industrial application if the membrane properties could be changed so that they would no longer change when applied in an industrial application.

The final research goal of this project is to determine whether or not the results from the H_2S conditioning experiments are reversible using common CMS membrane techniques including long term vacuum exposure and long term exposure to positive CO_2 pressure.

1.6 Thesis Organization

This thesis is divided into six chapters including this introduction chapter. The description of each of the chapters is as follows: Chapter 2 provides a background into CMS membranes, Chapter 3 describes the materials and experimental methods used throughout this research project, Chapter 4 identifies the steady state separation properties of Matrimid® derived CMS membranes and describes the results of the H_2S conditioning experiments, and Chapter 5 summarizes the research objectives and

accomplishments made through this work. The final chapter also makes recommendations for future work in the related areas of acid gas removal research.

1.7 References

[1]   United States Energy Information Administration. Office of Integrated Analysis and Forecasting. *International Energy Outlook 2011* http://www.eia.gov/forecasts/ieo/pdf/0484(2011).pdf. Date accessed, July 1st, 2012.

[2] United States Energy Information Administration. Office of Integrated Analysis and Forecasting. *International Energy Outlook 2012* http://www.eia.gov/forecasts/aeo/pdf/0383(2012).pdf. Date accessed, July 1st, 2012

[3]   Baker RW, Lokhandwala K. Natural gas processing with membranes: an overview. Ind & Eng Chem Research 2008; 47(7):2109-2121.

[4]   Bessho N. Advanced pressure swing adsorption system with fiber sorbents for hydrogen recovery. Atlanta GA USA, Georgia Institute of Technology, 2010.

[5]   Tabe-mohammadi A. A review of the applications of membrane separation technology in natural gas treatment. Separation Science and Technology 1999; 34(10):37-41.

[6]   Kiyono M. Carbon molecular sieve membranes for natural gas separations. Atlanta GA USA, Georgia Institute of Technology, 2010.

[7]   Robeson LM. Correlation of separation factor versus permeability for polymeric membranes. J Membr Sci 1991;62(2):165-185.

CHAPTER 2

BACKGROUND AND THEORY

2.1 Structure of CMS Membranes

Carbon molecular sieve (CMS) membranes are formed by heating an appropriate polymer precursor material above its decomposition temperature in a controlled environment in a process known as pyrolysis. The resulting material is nearly pure carbon [1,2]. When a polymer material is thermally decomposed the remaining carbon structure is either char or coke. The majority of CMS membranes are from polymer precursors that form char upon thermal decomposition. Char is an amorphous structure that is believed to have a largely aromatic structure comprised of graphene sheets with little order to the "stacking" of these graphene sheets. This stacking is not crystalline and is illustrated in Figure 2.1. The imperfect stacking of graphene sheets leaves "slit-like" pores which serve as idealized pores. This idealized pore structure model is shown in Figure 2.2 with the model's characteristic dimensions. The pore sizes in CMS membranes are represented

(a)   (b)
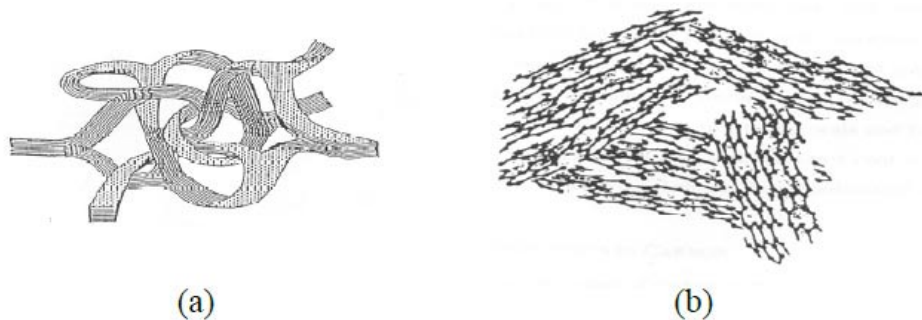
Figure 2.1: The amorphous stacking of graphene sheets, adapted from (a) Jenkins and Kawamura [2] and (b) Pierson [1].

by a bimodal pore size distribution similar to the one shown in Figure 2.2. The ultramicropore, pores with dimensions <7Å, is highly active during CMS formation, and it

has been shown that oxygen chemisorbs to this active site during pyrolysis that decreases the characteristic dimension, d_c [13].
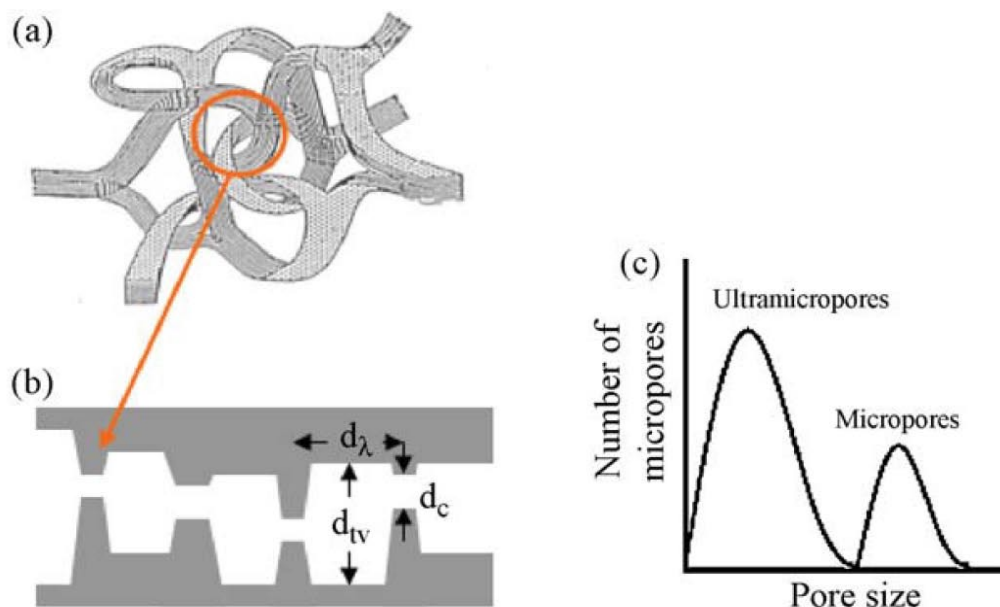
Figure 2.2: The amorphous stacking of graphene sheets (a), the idealized pore structure model with characteristic lengths of the micropores (b): d_λ represents the jump length dimension, d_{tv} represents the transverse dimension of the micropore, d_c is the micropore dimension, and the bimodal pore size distribution.

2.2 Formation of CMS Membranes

The separation properties of CMS membranes are dependent on several variables: the polymer precursor, the pyrolysis temperature, the thermal soak time, and the pyrolysis atmosphere.

2.2.1 Polymer Precursor

Jones and Koros [7] have suggested that polyimide precursor materials are the best available precursors for CMS membrane formation based on their separation properties and mechanical strength, although CMS membranes have been formed from polyimides [7], polyetherimide [8,9], and cellulose based materials [10]. Previous

researchers from the Koros group have investigated natural gas separations using various polyimide precursors. Vu showed that under identical pyrolysis conditions the CMS performance was highly dependent upon the polymer precursor used[6]. This conclusion was also affirmed through research performed by Williams [3] and Kiyono [4].
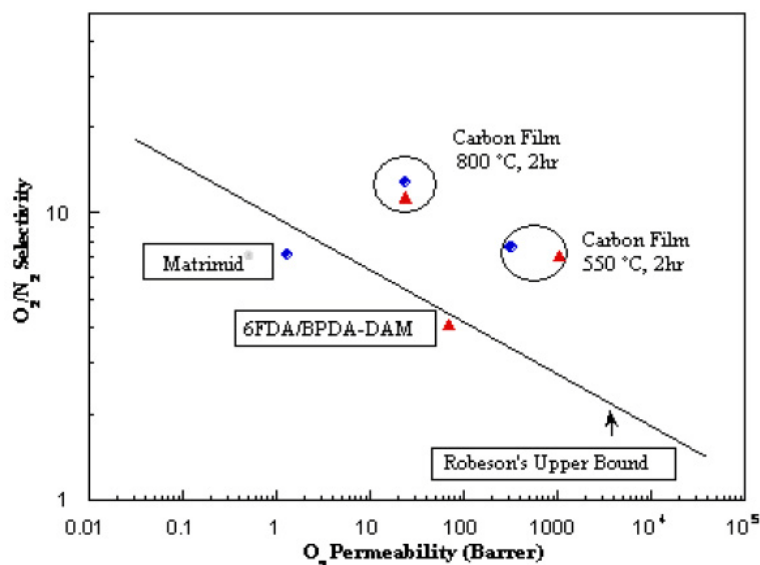
Figure 2.3: Transport properties of CMS membranes produced from two different polyimide polymer precursors. Notice the large difference in CMS properties depending on the precursor material, especially at 550 °C, adapted from [5].

2.2.2. Pyrolysis Temperature

The pyrolysis temperature refers to the highest temperature in the pyrolysis protocol. This temperature is referred to as the "soak temperature;" it is the temperature at which the polymer is held at for a defined time period. The pyrolysis temperature must lie between the thermal decomposition temperature and the temperature at which coke starts forming (typically ~2000 °C). As the pyrolysis temperature increases, the permeability of the CMS membrane decreases with an increase in selectivity as shown in Figure 2.3. At higher pyrolysis temperatures there is a shift in the size distribution of ultramicropores to smaller dimensions which gives rise to this trend for CO_2/CH_4 separations. This trend has been demonstrated repeatedly by various researchers [5, 6,

11]. These significant differences in separation properties as a function of pyrolysis temperature are shown in Figure 2.3, 2.4, and 2.6.

2.2.3 Thermal Soak Time

As previously mentioned the thermal soak time is the duration the precursor is held at the pyrolysis temperature. The thermal soak time can be adjusted to tune the separation characteristics of CMS membranes. Longer thermal soak times lead to an increased density of ultramicropores, and therefore, smaller permeabilities and larger selectivities. Steel has shown that while this trend holds true, the effect of the thermal soak time is dependent upon the the pyrolysis temperature [5]. At higher temperatures, >800 °C, the thermal soak time has a much larger impact on the permeability than it does on the selectivity compared to the effect an identical thermal soak time has on a lower temperature pyrolysis [5].
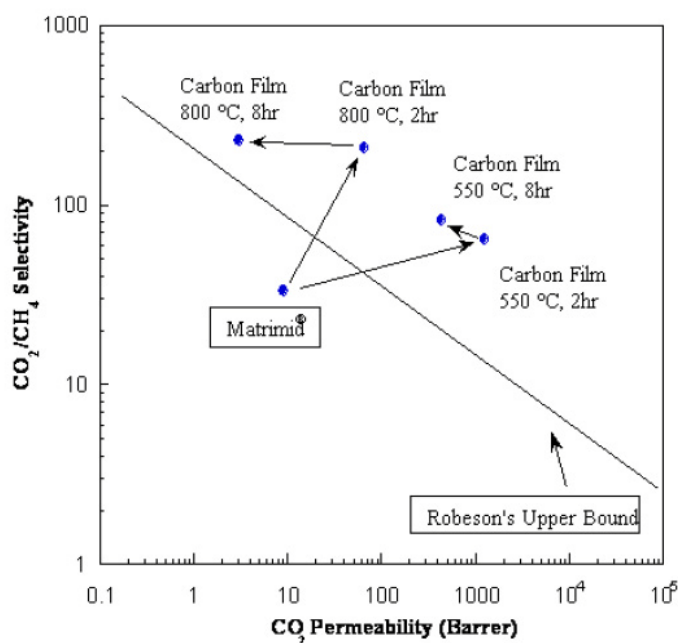
Figure 2.4: Separation properties of CMS membranes produced from Matrimid®. Both the effects that pyrolysis temperature and soak time are shown, adapted from Steel [5].

<u>2.2.4 Pyrolysis Atmosphere</u>

Kiyono looked extensively at the effects different inert and ppm level oxygen pyrolysis atmospheres may have on CMS separation properties [12]. Her results show that the oxygen content present in the pyrolysis atmosphere has an impact on the separation properties of the resulting CMS membrane. Oxygen present during pyrolysis "dopes" the ultramicropores via chemisorption resulting in a change in separation properties. Kiyono showed that the oxygen doping is equilibrium limited during the pyrolysis step. Figure 2.5 shows the tested hypothesis concerning oxygen doping of ultramicropores during the pyrolysis experiment. In the first case the CMS is optimally doped and there is a subsequent increase in selectivity and a decrease in permeability. The second case illustrates an overdoped case where the ultramicropore size has been decreased too much and both the selectivity and permeability have decreased. Figure 2.6 illustrates the effect oxygen doping can have on CMS membranes with two different pyrolysis temperatures. Matrimid® pyrolyzed at 550 °C is "overdoped," as there is a significant decrease in both permeability and selectivity as the amount of oxygen doped is increased. The data from Matrimid® pyrolyzed at 500 °C shows that the CMS is optimally doped with 30 ppm O_2, and it becomes overdoped upon pyrolysis in an atmosphere containing 50 ppm O_2 or more.

2.3 Transport in CMS Membranes

Gas transport in CMS membranes is modeled by the solution-diffusion mechanism. The solution-diffusion model describes gas permeation as the product of the solubility coefficient of the gas-membrane system and the diffusion coefficient of the gas penetrant through the membrane. Gas molecules will sorb into the membrane at the high pressure upstream and then diffuse across the membrane to the low pressure downstream due to the chemical potential gradient that exists across the membrane.
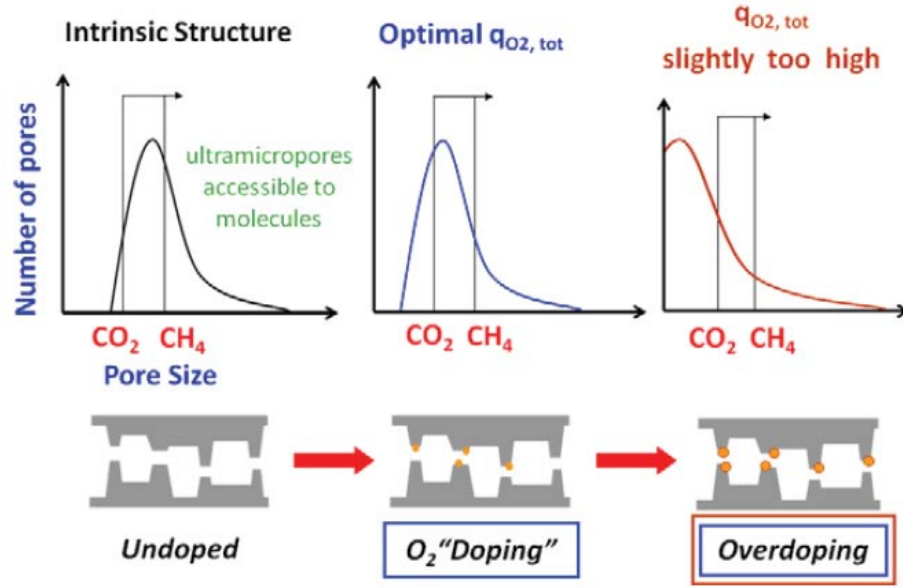
Figure 2.5: Oxygen doping model illustrating how oxygen doping can alter the ultramicropore structure [12].

There are two quantities that describe a membrane's separation properties, the permeability and the selectivity. The permeability is defined as the flux of the gas normalized by the thickness of the membrane and the pressure. Permeability is a measure of the intrinsic productivity of a given membrane. The definition of permeability can be found in Equation 2.1 below. The unit for permeability is the Barrer, and it is defined in Equation 2.2.

$$P_i = S_i \cdot D_i = \frac{n_i \cdot l}{\Delta p_i} \qquad \qquad 2.1$$

In Equation 2.1, P_i represents the permeability of component "i", S_i is the solubility of component i, D_i is the diffusivity of component i, n_i is the flux of component i through the
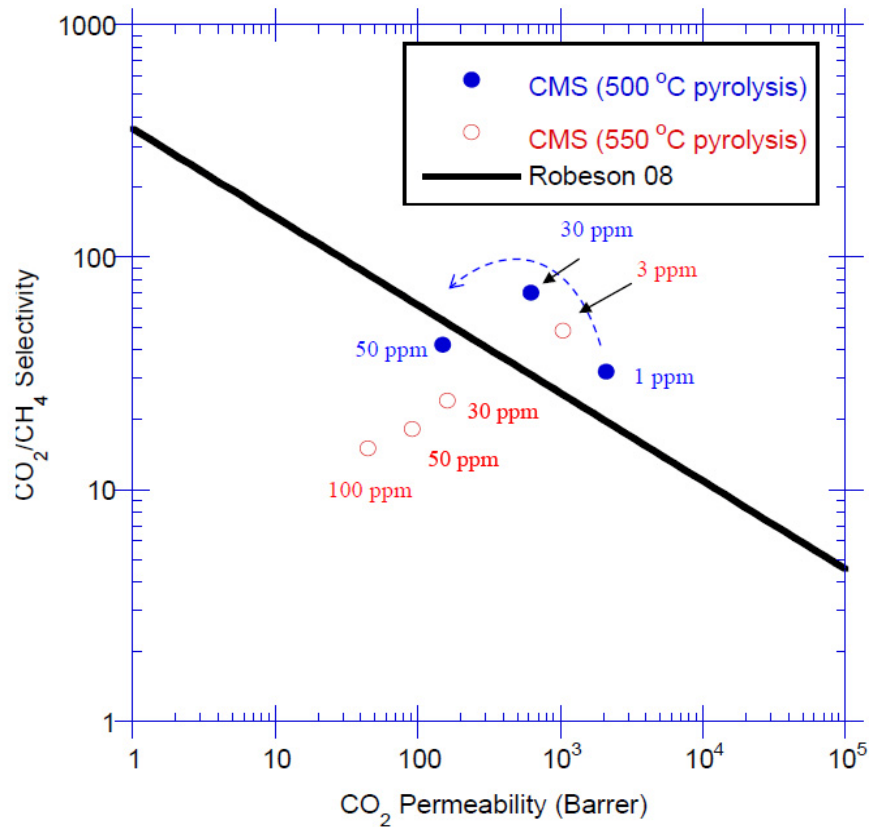
Figure 2.6: Separation performances of Matrimid® CMS dense films, adapted from Kiyono [4]. Note the significant difference in performance between O_2 doped Matrimid® at 500 °C vs 550 °C.

membrane of thickness, l, and Δp_i is the transmembrane partial pressure gradient which is the driving force for separation.

$$1 \, Barrer [=] 10^{-10} \frac{cm^3 (STP) \cdot cm}{cm^2 \cdot s \cdot cmHg} \qquad 2.2$$

For asymmetric hollow fiber membranes the thickness, "l," of the membrane is difficult to accurately and precisely measure so another unit convention is used. For asymmetric membranes the gas productivity is reported as the permeance instead of the permeability. The permeance of a membrane is the flux of the gas normalized by the

pressure gradient across the membrane. The definition of permeance can be found in Equation 2.3 below. The units of permeance are shown below in Equation 2.4.

$$\left(\frac{P}{l}\right)_i = \frac{n_i}{\Delta p_i} \qquad 2.3$$

$$1 \; GPU \; [=] \; 10^{-6} \frac{cm^3(STP)}{cm^2 \cdot s \cdot cmHg} \qquad 2.4$$

The selectivity is the separation efficiency of the membrane, and the ideal selectivity is defined as the ratio of the pure gas permeabilities. The selectivity is represented in equation form in Equation 2.5 below. The selectivity can also be subdivided into the product of ratio of the solubility coefficients (the sorption selectivity) and the ratio of the diffusivity coefficients (the mobility selectivity).

$$\alpha_{ij} = \frac{P_i}{Pj} = \frac{S_i \cdot D_i}{S_j \cdot D_j} \qquad 2.5$$

2.4 References

[1] Pierson HO. Handbook of carbon, graphite, diamond, and fullerenes. New York: Noyes Publication; 1993.

[2] Jenkins GM, Kawamura K. Polymeric carbons – carbon fiber, glass and char. London: Cambridge University Press; 1976.

[3] Williams PJ. Analysis of factors influencing the performance of CMS membranes for gas separation. Atlanta GA USA, Georgia Institute of Technology, 2006.

[4] Kiyono M. Carbon molecular sieve membranes for natural gas separations. Atlanta GA USA, Georgia Institute of Technology, 2010.

[5] Steel KM. Carbon membranes for challenging gas separations. Austin TX USA, The University of Texas at Austin, 2000.

[6] Vu DQ. Formation and characterization of asymmetric carbon molecular sieve and mixed matrix membranes for natural gas purification. Austin TX USA, The University of Texas at Austin, 2001.

[7] Jones CW, Koros WJ. Carbon molecular sieve gas separation membranes-I. Preparation and characterization based on polyimide precursors. Carbon 1994; 32(8):1419-1425.

[8] Sedigh MG, Jahangiri M, Liu PK, Sahimi M, Tsotsis TT. Structural characterization of polyetherimide-based carbon molecular sieve membranes. AICHE J 2000; 46(11):2245-2255.

[9] Sedigh MG, Xu L, Tsotsis TT, Sahimi M. Transport and morphological characteristic of polyetherimide-based carbon molecular sieve membranes. Ind Eng Chem Res 1999; 37:3367-3380.

[10] Koresh JE, Soffer A. Molecular sieve permselective membrane. Part I. Presentation of a new device for gas mixture separation. Sep Sci Technol 1983; 18(8):723-34.

[11] Barsema JN, Vegt NFA, Koops GH, Wessling M. Carbon molecular sieve membranes prepared from porous fiber precursor. J Membr Sci 2002; 205(1-2):239-246.

[12] Kiyono M, Williams PJ, Koros WJ. Effect of pyrolysis atmosphere on separation performance of carbon molecular sieve membranes. J Membr Sci 2010; 359(1-2):2-10.

[13] Williams PJ. Analysis of factors influencing the performance of CMS membranes for gas separations. Atlanta GA USA, Georgia Institute of Technology, 2006.

CHAPTER 3

MATERIALS AND EXPERIMENTAL PROCEDURES

3.1 Introduction
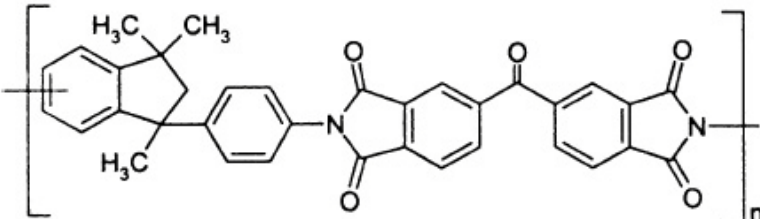
This chapter provides the information regarding the materials used to produce the carbon molecular sieve (CMS) membranes used throughout this study. The experimental procedure followed to formulate working modules is also described. The H_2S testing protocols are outlined in detail, and the methods used to obtain gas permeation data are also described.

3.2 Materials

3.2.1 Polymer

CMS membranes are formed by heating the polymer precursor material above its decomposition temperature. The commercially available polymer Matrimid® 5218 (BPTI-DAPI) was used in this study since its transport properties have been studied extensively [1]. Previous researchers have analyzed this polymer precursor due to its low cost and availability for possible industrial scale-up in the future. The Matrimid® polymer was purchased from Huntsman International LLC. Its chemical structure and properties can be found in Table 3.1. The polymer was dried at 110 °C under vacuum to remove moisture and organic volatiles before using it to prepare a dope.

Table 3.1: Chemical Structure and Properties of Matrimid® 5218 [2,3]. T_g represents the glass transition temperature and T_d represents the thermal decomposition temperature.

Chemical Structure	T_g [°C]	T_d [°C]
	315	425

All pure gases used, excluding H_2S, were provided by Air Gas and were ultra high purity or research grade (minimum purity of 99.999%). Pure gas hydrogen sulfide was provided by Praxair. The argon mixed gases used for inert pyrolysis were provided by Air Gas and contained ppm level oxygen (1.05-27.4 ppm O_2) in Argon as specified. Two separate acid gas mixtures were used in this study and were provided by Praxair. The first mixed gas contained 20.0 mol % H_2S, 20.0 mol % CO_2, and a balance of CH_4 while the second mixed gas contained 5.0 mol % H_2S, 45.0 mol % CO_2, and a balance of CH_4.

3.2.3 Solvents

The solvents used for dope formation and spinning were all purchased from Sigma Aldrich and were all anhydrous, 99.5% purity. The solvents used for solvent exchange were all solvent grade and were purchased from VWR International.

3.3 CMS Hollow Fiber Membrane Formation

3.3.1 Asymmetric Hollow Fiber Membrane Formation

Asymmetric hollow fiber membranes are the industrial preferred geometry for membranes for gas separations due to their high surface area to volume ratio. Asymmetric hollow fiber membranes are fabricated by a co-extrusion process known as spinning. Two fluids, a "dope" and a "bore fluid" are co-extruded through a spinneret. The dope consists of the polymer material, a solvent, and a non-solvent. The dope composition is dependent upon the polymer-solvent system being used. The dope is formulated so that the dope composition lies close to the binodal line on the ternary phase diagram. It's important for the dope composition to lie as close to the binodal composition as possible because there should only be enough solvent to allow phase separation in the air gap during the spinning process. The ternary phase diagram and a brief explanation can be found in Figure 3.1.

The asymmetric precursor hollow fiber membranes used in this study were formed by a dry-jet/wet-quench spinning process. In the dry-jet/wet-quench spinning process the dope and bore fluids are co-extruded into an air-gap before being quenched in an aqueous bath. A schematic of the dry-jet/wet-quench spinning process can be found in Figure 3.2. The dope formulation was prepared as described by Clausi and Koros by another Koros Group Member – Nitesh Bhuwania [7]. The dope was placed on a roller at room temperature until the dope appeared homogeneous by inspection or 4 weeks in this case.   Once the dope was homogeneous the dope was loaded into a 500 mL syringe pump and allowed to degas overnight before the spinning process was performed.

Following completion of the spinning process a solvent exchange process is performed to avoid collapse of the porous substructure. The fibers were soaked in three separate deionized water baths inside vertical glass containers for 24 hours per water bath. The fibers were then placed in three separate methanol baths for 20 minutes per bath followed by three 20 minute hexane baths. After the solvent exchange process was completed the fibers were dried under vacuum at 80 °C for 2 hours. Once the entire process has been completed the fibers were stored in a plastic bag with a desiccant pouch to remove moisture from the bag atmosphere.

A → A': skin formation in the air gap

A → B: substrucutre formation in the quench bath
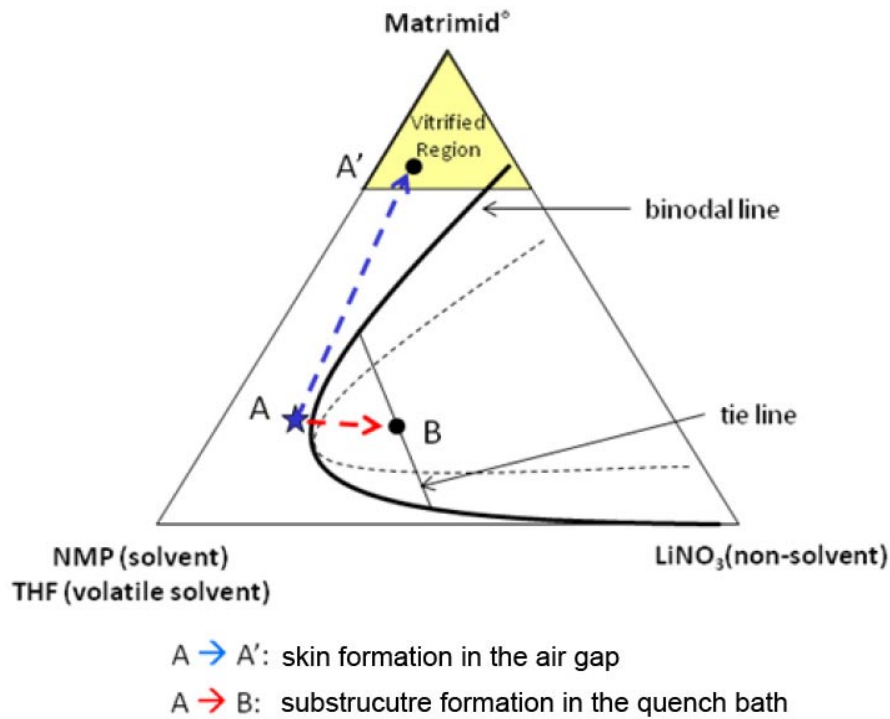
Figure 3.1: Ternary diagram of the dope composition during the spinning process. Point A represents the dope composition prior to spinning. Point A' represents the dense skin layer of the hollow fiber membrane. Point B represents the porous substructure of the hollow fiber membrane. Adapted from [1].
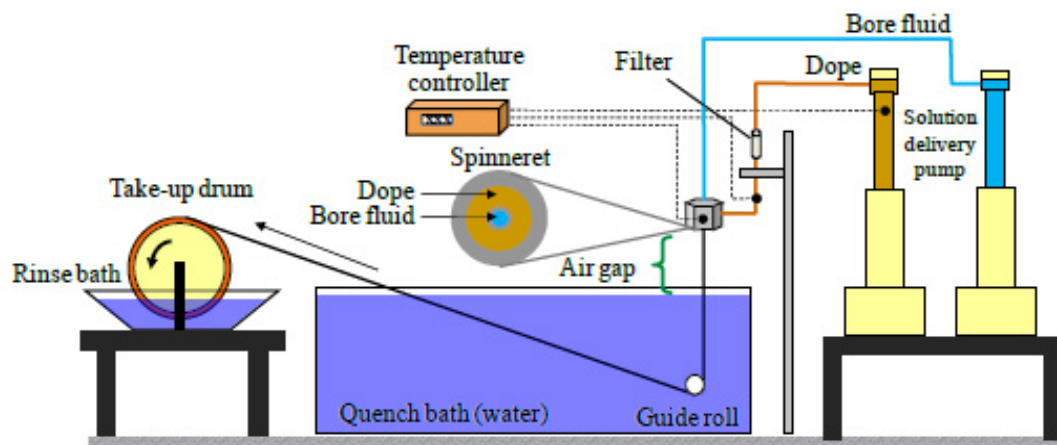
Figure 3.2 Schematic of dry-jet/wet-quench spinning process. Dry-jet/wet-quench spinning is the process used to produce polymer precursor asymmetric hollow fiber membranes.

<u>3.3.2 Extended Solvent Exchange</u>

An additional solvent exchange step was carried out in an attempt to "heal" any minor surface defects on the fibers. The fibers were rewetted with DI water for 24 hours. The fibers were then soaked in three consecutive methanol baths for 24 hours per bath before finally soaking in three 24 hour hexane baths. Similar to post-spinning solvent exchange, the fibers were finally dried under vacuum at 80 °C for 2 hours.

3.4 CMS Membrane Formation

The production of CMS membranes from polymer precursors was performed as indicated by previous researchers [10,11]. In our case, there have been slight improvements to the temperature and atmosphere control within the pyrolysis furnace as outlined by Xu and Rungta [12]. A three zone furnace manufactured by Thermocraft, Inc. (model XST-3-0-24-3C) was used for the pyrolysis experiment. Each of the three zones was controlled separately by a multi-channel temperature controller manufactured by Omega Engineering, Inc. (model CN1504TC). The control sensors used were thermocouples manufactured by Marlin Manufacturing Corp. The sample for pyrolysis was enclosed within a quartz tube supplied by National Scientific Company and sealed with a silicon O-ring and metal flange assembly similar to those previously reported [1,12]. The hollow fiber membranes were supported within the quartz tube by a stainless steel perforated plate supplied by McMaster Carr and held in place on the plate with thin wires. A schematic of the three zone pyrolysis furnace can be viewed in Figure 3.3.

The separation properties of CMS membranes are a function of both polymer precursor and the pyrolysis conditions. Previous research has shown that CMS membranes produced from Matrimid® precursors do not show industrially favorable oxygen doping when pyrolyzed at higher temperatures [1,4]. Kiyono showed that

23

Matrimid® CMS membranes pyrolyzed and oxygen doped at 550 °C do not have a higher selectivity than those without oxygen doping. It was shown that the oxygen doping that takes place during pyrolysis at 550 °C causes a significant drop in both selectivity and permeability. It was shown however, that Matrimid® CMS membranes pyrolyzed and oxygen doped at 500 °C exhibit more favorable separation properties. Therefore, a final pyrolysis soak temperature of 500 °C was used in this study. The furnace was heated until each zone was 50 °C and once the zones reached 50 °C, the
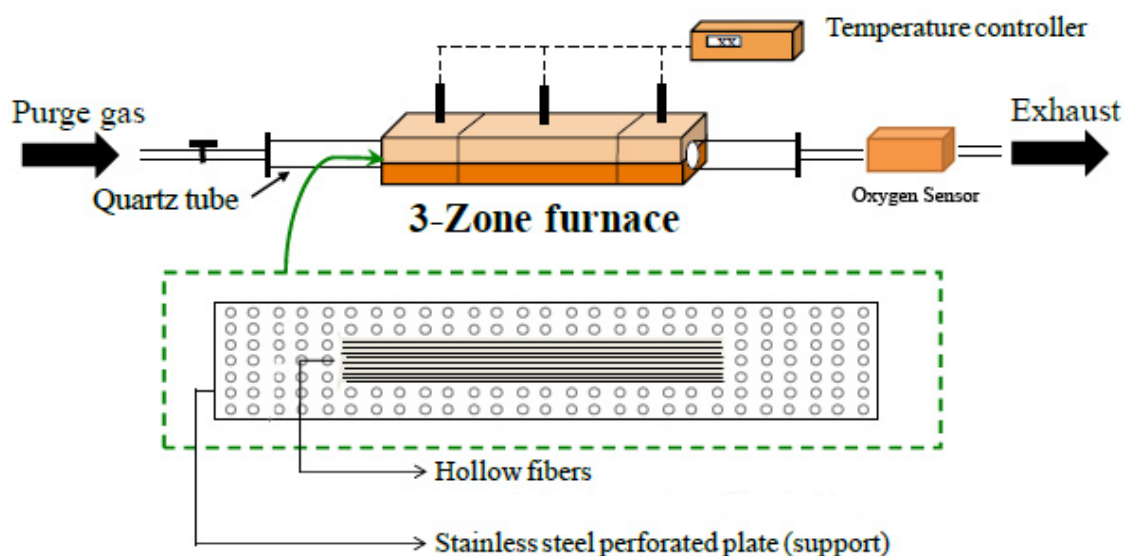
Figure 3.3: Schematic of the 3-zone furnace used to pyrolyzed hollow fiber membranes adapted from Chen [17].

temperature protocol found in Table 3.2 was used. After each pyrolysis experiment the quartz tube and stainless steel mesh plate were cleaned thoroughly with acetone and then burned out at 800 °C to remove any left-over pyrolysis by-products from the surfaces. The temperature protocol for the burn out procedure can be found in Table 3.3.

Table 3.2: Pyrolysis protocol used for the formulation of CMS hollow fiber membranes from Matrimid® precursor fibers. The ramp rates used are the same as previous researchers and Step 4 indicates a thermal soak at the final pyrolysis temperature.

	Start Temperature [°C]	End Temperature [°C]	Time to End Temperature [min]
Step 1	50	50	20
Step 2	50	250	15
Step 3	250	485	61
Step 4	485	500	60
Step 5	500	500	120

Table 3.3: Temperature protocol used for the burning out of experimental equipment following the pyrolysis of polymer precursors.

	Start Temperature [°C]	End Temperature [°C]	Time to End Temperature [min]
Step 1	50	50	20
Step 2	50	800	80
Step 3	800	800	120

3.5 Hollow Fiber Permeation

3.5.1 Module Making

The CMS hollow fiber membranes were made into modules according to previous researchers [1,13,14]. The modules used in this work consisted of a single fiber with an active length of approximately 10 cm for each module. Due to the highly aggressive nature of the gas mixtures used in this work, a high temperature, chemically resistant epoxy was used in place of the typical 5 minute epoxy (DP(100)) which is used for many hollow fiber membrane modules. Duralco 4461 epoxy manufactured by Cotronics Corp.

was used as the chemically resistant epoxy. This epoxy offers chemical resistance even at high temperatures (500 °F). As this was not a high temperature application and to limit the CMS membrane exposure to further high temperatures, the additional high temperature curing instructions were not used. The epoxy was simply allowed to cure at room temperature for at least 24 hours.

3.5.2 Pure Gas Permeation

All pure gas permeation experiments were carried out using a constant volume permeation system. These permeation systems are described in detail elsewhere [11,15,16]. The permeation box is enclosed and well insulated to minimize heat transfer to the surroundings. A schematic of the constant volume-variable pressure permeation system used in this work can be found in Figure 3.4. An additional modification was made to this permeation system when compared to other permeation systems previously reported in the literature. There is a house nitrogen line that is used to constantly purge and circulate the air on the inside of the permeation system while the membrane module is exposed to H_2S. This was designed as a safety measure to prevent the buildup of H_2S inside the permeation system during prolonged H_2S conditioning and permeation experiments.

Before any permeation experiments were carried out, membrane modules were degassed by pulling vacuum on both the shell and bore side of the module for a minimum of 12 hours. After degassing, a leak test was performed to ensure the leak rate was <1% of the permeate rate of the slowest gas, CH_4 in this case. A leak test also ensures that the downstream is efficiently sealed from the atmosphere and that the membrane is successfully degassed. If the leak test showed gas-desorption, then additional time under vacuum was required to degas the module.
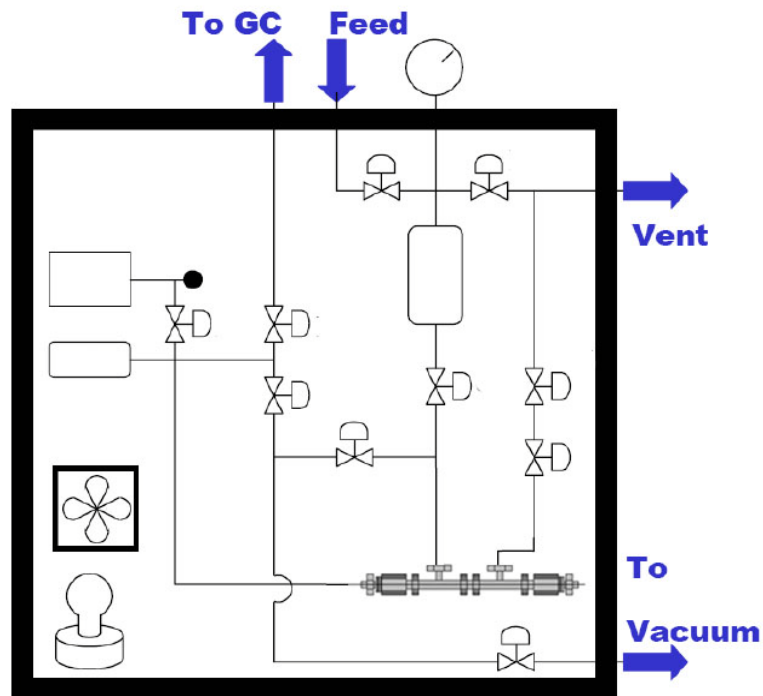
Figure 3.4: Schematic of a constant volume hollow fiber permeation system, adapted from Moore et al [18].

The pure gas CO_2 and CH_4 permeation experiments were carried out at 250 psia with a shell side feed. The upstream pressure inside the permeation system was measured with a Honeywell STJE pressure transducer (calibrated from 0-1500 psia). The downstream pressure (dp/dt) rise was recorded by LabView from an MKS Baratron® Type 121A pressure transducer (calibrated from 0-100 torr). The permeation of the gas through the membrane can be calculated using equation 3.1 where dp/dt is the pressure rise in torr/s, V_R is the downstream volume in cm^3, A_c is the surface area of the hollow fiber membrane in cm^2, and Δp is the transmembrane pressure in psi. The calculated permeance is in gas permeation units (GPU).

$$\left(\frac{P}{l}\right) = \frac{(2.25 \times 10^3) \cdot V_R}{A_c \cdot \Delta p} \cdot \left(\frac{dp}{dt}\right)$$ 3.1

3.6 H$_2$S Conditioning Protocols

All H$_2$S conditioning experiments were carried out with two 1 L syringe pumps in parallel. Utilizing both pumps allowed the user to operate at the high pressures of pure and mixed gas feeds required for these experiments.

3.6.1 Extended Conditioning

The extended conditioning protocol was meant to represent the most aggressive natural gas reserves in the world and the impact they could have on a fresh CMS membrane module. The extended conditioning protocol involves a 24 hour soak with 1135 psia mixed gas: 20.0 mol % H$_2$S, 20.0 mol % CO$_2$, 60.0 mol % CH$_4$. After soaking, the temperature inside the permeation system was increased to 50 °C and the entire hollow fiber module (both shell and bore side) were under active vacuum for at least 24 hours to completely desorb any remaining condensable gases. While developing this protocol, in an attempt to ensure complete desorption of H$_2$S, a leak test was performed for extended periods of time (in excess of 6 hours) to check for desorption in the downstream. Once the module had been completely desorbed the permeation system was set back to 35 °C before performing the next pure gas permeation experiment.

3.6.2 Rapid Conditioning

As previously mentioned, a rapid conditioning protocol was chosen in an attempt to quickly condition the CMS membranes to their steady state permeation properties. The rapid conditioning approach was chosen as an alternative conditioning approach, so the conditioned transport properties could be measured accurately with two separate conditioning protocols, keeping the control variable constant, H$_2$S activity. The rapid conditioning protocol involves a 24 hour soak at 150 psia pure H$_2$S on the upstream (shell) side of the module while the downstream (bore) side of the module is still under active vacuum. Similar to the extended conditioning protocol, after a 24 hour soak the temperature inside the permeation system was increased to 50 °C and the entire hollow

fiber module (both shell and bore side) were under active vacuum for at least 72 hours to completely desorb any remaining H_2S. After this desorption step, the temperature inside the permeation system was set back to 35 °C and the system was allowed to reach equilibrium. Once the system had reached equilibrium another pure gas permeation experiment could begin.

3.7 Scanning Electron Microscope (SEM)

SEM images were obtained in order to calculate the outer diameter, (and therefore the surface area), of the CMS hollow fiber membranes used in each module. The fibers were prepared by cleanly fracturing the CMS membranes leaving a relatively flat surface to be imaged. The hollow fibers were oriented on an SEM tray so that the image obtained was that of the end of the hollow fiber. The SEM used in this study was a LEO 1530 thermally assisted field emission (TFE) SEM.

3.8 Fourier Transform Infrared (FTIR) Spectroscopy

The FTIR experiments were carried out using a Bruker Tensor 27 FTIR spectrometer. For the CMS samples, the CMS fibers were crushed into a powder after transport studies were completed. Samples were analyzed using a Harrick MVP2 micro ATR with 128 scans at a resolution of 2 cm^{-1}.

3.9 References

[1] Kiyono M. Carbon molecular sieve membranes for natural gas separations. Atlanta GA USA, Georgia Institute of Technology, 2010.

[2] Vu DQ, Koros WJ, Miller SJ. Mixed matrix membranes using carbon molecular sieves-I. Preparation and experimental results. J Membr Sci 2003; 211(2):311-334.

[3] Vu DQ, Koros WJ, Miller SJ. Mixed matrix membranes using carbon molecular sieves-II. Modeling permeation behavior. J Membr Sci 2003; 211(2):335-348.

[4] Kiyono M, Williams PJ, Koros WJ. Effect of polymer precursors on carbon molecular sieve structure and separation performance properties. Carbon 2010; 48(15):4432-4441.

[5] Pesek SC, Koros WJ. Aqueous quenched asymmetric polysulfone membranes prepared by dry/wet phase separation. J Membr Sci 1993; 81:71-88.

[6] Pesek SC, Koros WJ. Aqueous quenched asymmetric polysulfone hollow fibers prepared by dry/wet phase separation. J Membr Sci 1994; 1994:1-19.

[7] Clausi DT, Koros WJ. Formation of defect-free polyimide hollow fiber membranes for gas separations. J Membr Sci 2000; 167(1):79-89.

[8] Carruthers SB, Ramos GL, Koros WJ. Morphology of integral-skin layers in hollow fiber gas separation membranes. J Appl Polym Sci 2003; 90:399-411.

[9] McKelvey SA, Clausi DT, Koros WJ. A guide to establishing hollow fiber macroscopic properties for membrane applications. J Membr Sci 1997; 124:223-32.

[10] Kiyono M, Williams PJ, Koros WJ. Effect of pyrolysis atmosphere on separation performance of carbon molecular sieve membranes. J Membr Sci 2010; 359(1-2):2-10.

[11] Vu DQ, Koros WJ, Miller SJ. High pressure CO_2/CH_4 separation using carbon molecular sieve hollow fiber membranes. Ind Eng Chem Res 2002; 41(3):

[12] Xu LR, Rungta M, Koros WJ. Matrimid (R) derived carbon molecular sieve hollow fiber membranes for ethylene/ethane separation. J Membr Sci 2011; 380(1-2):138-147.

[13] Wallace DW. Crosslinked hollow fiber membranes for natural gas purification and their manufacture from novel polymers. Austin TX USA, University of Texas at Austin, 2004.

[14] Kosuri MR, Koros WJ. Defect-free asymmetric hollow fiber membranes from Torlon (R), a polyimide-imide polymer, for high-pressure CO_2 separations. J Membr Sci 2008; 320(1-2):65-72.

[15] Pye DG, Hoehn HH, Panar M. Measurement of gas permeability of polymers. 1. Permeabilities in constant volume/variable pressure apparatus. J Appl Polym Sci 1976; 20(7):1921-31

[16] Pye DG, Hoehn HH, Panar M. Measurement of gas permeability of polymers. 2. Apparatus for the determination of permeabilities of mixed gases and vapors. J Appl Polym Sci 1976; 20(2):287-301

[17] Chen CC. Thermally crosslinked polyimide hollow fiber membranes for natural gas purification. Atlanta GA USA, Georgia Insititute of Technology, 2011.

[18] Moore TT, Damle S, Williams PJ, Koros WJ. Characterization of low permeability gas separation membranes and barrier materials; design and operation considerations. J Mem Sci 2004; 245(1-2): 227-231.

CHAPTER 4

RESULTS AND DISCUSSION

4.1 Introduction

In this chapter the data and results for H_2S conditioning, which comprised the key experimental thrust of this thesis, are presented. Both the extended conditioning and rapid conditioning protocols used a feed gas with the same activity of H_2S. The CMS membranes used in the initial experiments were pyrolyzed in an Ar inert atmosphere with 2 ppm O_2 using the standard 500 °C pyrolysis protocol. Follow up experiments were performed using CMS membranes with various oxygen doping from 2-29 ppm O_2 in Ar. Recall that 500 °C was used for the pyrolysis, since a 550 °C pyrolysis temperature with greater than 2 ppm O_2 was known to create a structure that was already too "tight" for CO_2/CH_4 separations. Any reaction at the size discriminating ultramicropores is expected to result in undesirable shutdown of permeability, this is the case for oxygen doping at 550 °C.

4.2 H_2S Conditioning

As previously mentioned in Chapter 1, preliminary data from previous Koros Group researchers noticed a significant change in transport properties as CMS membranes were exposed to H_2S. These changes in transport properties are being described as H_2S conditioning. The previous exposure was limited to a mixed feed of 10 mol% H_2S with a CH_4 balance at 50 psia (35 °C), which was considered a modest exposure to H_2S. Also as previously mentioned the goal of this project is to identify the extent that H_2S permeability changes as a function of H_2S exposure time. The testing hypothesis was that H_2S conditioning for consecutive 24hr exposure times with constant H_2S activity would lead to stable steady state transport properties.

4.3 Extended Conditioning

The extended conditioning protocol, (Section 3.6.1), was chosen to model how an unconditioned CMS hollow fiber membrane module would respond upon exposure to aggressive sour gas wells. The feed concentration, (20.0 mol % H_2S, 20.0 mol % CO_2, 60.0 mol % CH_4), and testing pressure (1135 psia) were chosen to represent very aggressive natural gas wells. After each successive 24 hour soak, a pure gas CO_2 permeation experiment was used to monitor the change in permeability of the CMS membrane. Based on the previous research, we expected the pure gas permeances to decrease as a function of mixed gas exposure. Since the exact mechanism of H_2S transport in CMS is not yet known [1], the hope was that the pure gas permeances would approach a steady state value and not simply decrease indefinitely as the permeances do after H_2O exposure [1].

A pure gas CO_2 permeance experiment at 150 psia was carried out after each successive 24 hour exposure. A pure gas CH_4 permeance experiment carried out at 150 psia feed pressure after the CO_2 permeance approached the observable steady state. While the permeance of CO_2 decreased after conditioning with H_2S, it was determined that the CO_2/CH_4 selectivity increased. The initial and final transport properties can be found in Table 4.1.

As expected, there was a significant drop in permeance upon exposure to the high pressure mixed gas feed. The CO_2 permeation decreased significanly after just 24 hr exposure. As the number of consecutive 24 hr exposures increased, the decreasing CO_2 permeation rate slowed before reaching a steady state value after 120 hours. After 120 hours, the CO_2 permeation did not change within 3% of the previous CO_2 permeation value. The steady state permeation value is approximately 40% less than the unconditioned CMS membrane. The CO_2 permeation data is shown in Figure 4.1.
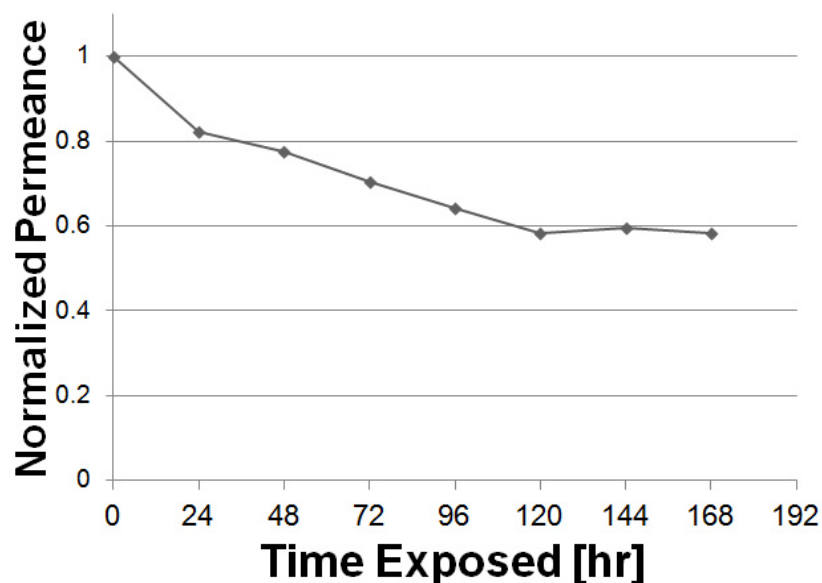
Figure 4.1: Pure gas CO_2 normalized permeation change as a function of time exposed to the extended conditioning mixed gas feed. Here the permeances are normalized by the pure gas CO_2 permeance of the unconditioned membrane. CMS hollow fiber membranes produced via pyrolysis at 500 °C with 2 ppm O_2 in Ar pyrolysis atmosphere.

Table 4.1: Permeance and selectivity of CMS membrane after H_2S exposure via the extended conditioning protocol.

Total H_2S Exposure	CO_2 Permeance	CO_2/CH_4 Ideal Selectivity
[hr]	[GPU]	[--]
0	8.4	16.4
144	5.0	26.7

These results indicate that part of our hypothesis is confirmed. The CMS membrane does approach a steady state upon sufficient exposure to H_2S. This confirmation suggests that an unconditioned membrane module in a highly aggressive natural gas purification process would reach a steady state where its transport properties did not change as a function of acid gas exposure.

4.4 Rapid Conditioning

The rapid conditioning protocol, (Section 3.6.2), was chosen as an alternative to the extended conditioning protocol. This alternative protocol was meant to model a final step in production that membrane manufacturers could perform before final delivery to the customer or natural gas processing site. The goal was to quickly condition an otherwise lengthy change to steady state properties as the extended conditioning or "module in industrial use" showed the membranes to undergo. As mentioned in Chapter 1, the rapid conditioning protocol involves a 24 hour soak at 150 psia pure H_2S on the upstream (shell) side of the module while the downstream (bore) side of the module is under active vacuum. Similar to the extended conditioning protocol, after each 24 hour soak a pure gas CO_2 permeation experiment was performed with a CO_2 upstream pressure of 150 psia.
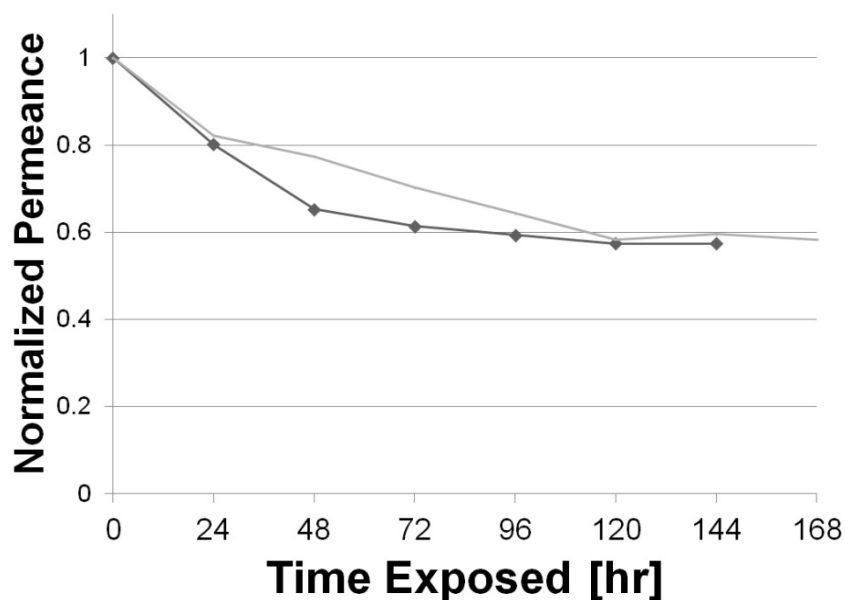
Figure 4.2: Pure gas normalized CO_2 permeation change as a function of time exposed to the rapid conditioning pure gas feed. The light curve represents the extended conditioning data. Here the permeances are normalized by the pure gas CO_2 permeance of the unconditioned membrane.CMS hollow fiber membranes produced via pyrolysis at 500 °C with 2 ppm O_2 in Ar pyrolysis atmosphere.

As expected, the rapid conditioning set of experiments also showed a decrease in CO_2 permeance as the time exposed to H_2S increased. There was a noticeable difference in the time it took for the change in CO_2 permeance to reach the proposed steady state. After 72 hours the CO_2 permeance had decreased by approximately 40% and the CO_2 permeance leveled out, to the same steady state characterized in the extended conditioning set of experiments. After 72 hours the CO_2 permeance remained unchanged within 3%, the same threshold used to determine the steady state in the extended conditioning set of experiments. This time period differs significantly from the 120 hour conditioning time required by the extended conditioning protocol. The CMS membranes had conditioned from an initial state with a CO_2 permeance of 17.6 GPU and a CO_2/CH_4 selectivity of 17.6 to a final state with a CO_2 permeance of 5.8 GPU and a CO_2/CH_4 selectivity of 25.4

The rapid conditioning set of experiments was repeated and the results confirmed the results from the initial set of experiments. One key difference in the second set of experiments was the final 30 minutes of each 24 hour soak was performed similar to a pure gas permeation experiment. The downstream vacuum valve was closed and the pressure rise in the downstream volume was recorded to calculate the pure gas H_2S permeance. The data from this rapid conditioning set of experiments is shown in Table 4.2. Once the final state is reached, the CO_2, H_2S, and CH_4 permeances of the CMS membranes do not change, as indicated by the H_2S/CH_4 selectivities in Table 4.2, as a function of H_2S exposure. These results, along with the extended conditioning results, confirm part of our hypothesis and indicate there is a second state where the transport properties no longer change as a function of H_2S exposure.

36

Table 4.2: Permeance and selectivity of CMS membrane after H_2S exposure via the rapid conditioning protocol. CMS membrane prepared pyrolysis at 500 °C with 2 ppm O_2 in Ar pyrolysis atmosphere.

Total H2S Exposure [hr]	CO_2 Permeance [GPU]	% Decrease in CO_2 Permeance [--]	CO_2/CH_4 Selectivity [--]	H_2S/CH_4 Selectivity [--]
0	10.1	--	17.6	--
48	6.5	35.7	24.8	15.6
96	6.0	40.7	25.3	16.0
120	5.8	42.6	25.4	15.9

4.5 Possible Mechanism for H_2S Conditioning

It has been shown that oxygen doping during pyrolysis affects the transport properties of CMS membranes. The schematic in Figure 4.3 illustrates the role oxygen doping has in the sieving of gas penetrants at ultramicropore sites [1,2,5]. Gas transport in CMS membranes is modeled via the solution-diffusion model as described in Chapter 2. The changes in transport properties measured with these experiments are therefore a representation of the product of the effects H_2S exposure has to both the solubility and diffusion of various molecules through the CMS membrane. The exact manner in which the conditioning of CMS membranes occurs is still unknown, but one hypothesis is that H_2S chemisorbs at both the micropore sorption sites and the ultramicropore sieving sites. The chemisorption of H_2S as represented in Figure 4.4 would accurately describe the observed data. The presence of chemisorbed H_2S at micropore sorption sites would decrease both the CO_2 and CH_4 sorption, and by extension the observed permeabilities. This decrease in the sorption capacity for pure gas permeation should increase as the H_2S exposure is increased which the data also supports. In Figure 4.4 state "b" would represent the membrane after 24-48 hour exposure to H_2S. The CO_2 permeation has

clearly decreased significantly after only 48 hours. State "c" represents the final, hypothetical conditioned state in which the available active ultramicropore sites become
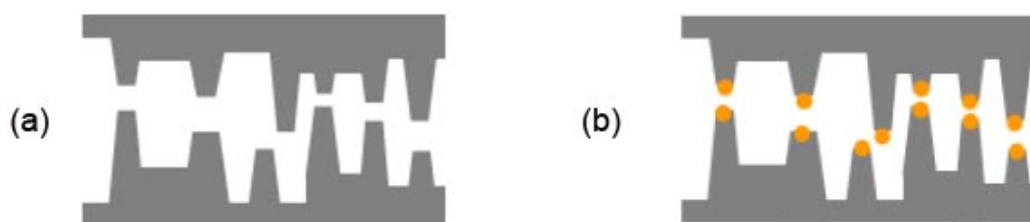
Figure 4.3: Schematic illustrating the CMS slit like structure both without (a) and with (b) oxygen doping. Adapted from Kiyono [2]. The oxygen doped CMS membrane has optimal transport properties.

saturated and there is no longer a change in transport properties observed. The sorption of H_2S at the ultramicropore sieving sites should decrease the overall ultramicropore size density and effectively sieve CH_4 molecules at sites that would not have sieved in an unconditioned membrane. These "new" selective pores would only be available to CO_2 diffusion and would therefore increase the mobility selectivity.

Figure 4.4: Schematic illustrating the CMS slit like structure from an oxygen doped membrane: (a) initial state, (b) partially conditioned state, (c) final, conditioned state.

In order to better describe or model the conditioning mechanism, more characterization data are required. Future sorption studies could provide information on the change in

solubility before, during, and after conditioning. Should the sorption of H_2S and CO_2 decrease after conditioning there will be also be a change in the sorption selectivity as well. This is discussed further in Chapter 5.

4.6 Modeling the H_2S Conditioning Reaction

The change in permeance observed as a function of H_2S exposure has been shown for both rapid H_2S conditioning and extended H_2S conditioning. Following both conditioning procedures leads to a conditioned state with similar transport properties, both conditioned states exhibit a ~40% drop in permeance. Since the H_2S activity in both conditioning procedures is the same, this supports our hypothesis that the conditioned state is a function of H_2S activity. A look at the rate of chemisorption that takes place upon H_2S exposure should provide insight into the kinetic limitations of H_2S conditioning.

The proposed rate law for H_2S chemisorptions is shown in Equation 4.1 where *[x]* represents the number of unreacted sites per cm^3 available for chemisorption. The number of unreacted sites cannot be readily measured. As has been described in this work, the number of active unreacted sites are believed to be proportional to the measured CO_2 permeance, allowing us to approximate the rate law and rate constant with the CO_2 permeance data using Equation 4.2.

$$\frac{d[x]}{dt} = -k \cdot [x]^n \qquad \text{4.1}$$

$$\frac{d\left(\frac{P}{l}\right)}{dt} = -k \cdot \left(\frac{P}{l}\right)^n \qquad \text{4.2}$$

Upon checking for first, second, and third reaction order rate, the data indicate a first order reaction rate, $n = 1$, and the calculated rate constants are shown in Table 4.3. The

rate constant for the rapid conditioning experiment more fundamentally describes the chemisorption rate of H_2S on CMS membrane active sites. The difference in observed reaction rate is most likely due to competitive sorption effects. In the extended conditioning mixed gas feed there are three gases present, of which two are highly condensable, CO_2 and H_2S. It is likely that CO_2 and to a lesser extent CH_4 compete for micropore sorption sites and decrease the observed rate of reaction compared to the pure gas rapid conditioning step.

Table 4.3: First order rate constants for the H_2S conditioning of CMS membranes produced from Matrimid® precursors produced by 500 °C pyrolysis in Ar with 2 ppm O_2 atmosphere.

Conditioning Protocol	Rate Constant, k
[--]	10^{-3} [s^{-1}]
Extended	4.7
Rapid	7.6
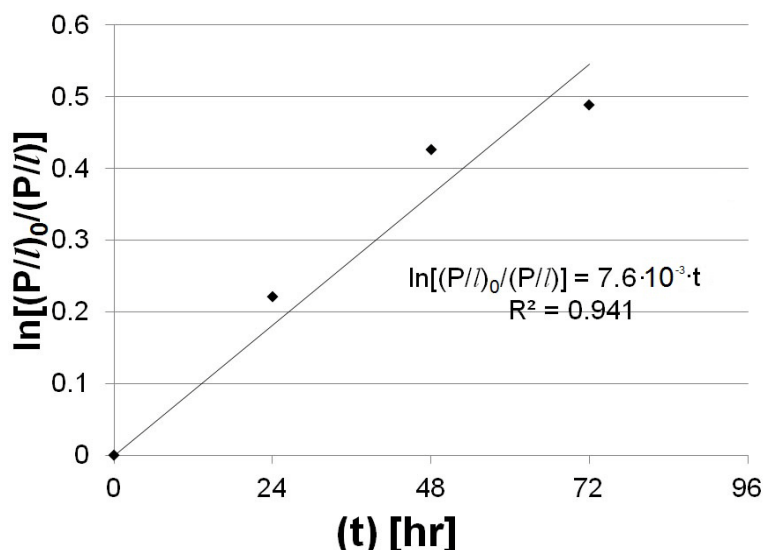
Figure 4.5: Integral Method plot used to calculate rate constants. The plot of $\ln[(P/l)_0/(P/l)]$ as a function of time yields a linear plot with slop k, the rate constant. The above data represent the rapid conditioning changes.

The FTIR results presented in Figure 4.5 indicate the change upon H_2S conditioning. The wavenumbers of interest lie between 1520-1000 cm^{-1} which indicate the presence of sulfur containing functional groups. According to the literature [19,20], the presence of a new absorbance peak at 1050 cm^{-1} in the conditioned membrane most likely corresponds to the presence of sulfoxide, S=O, functional groups that were not present in the unconditioned membrane. The presence of sulfoxide in the conditioned membranes also suggests the importance oxygen doping has on H_2S conditioning. The effects of oxygen doping on the H_2S conditioned state are further explored in Section 4.6.
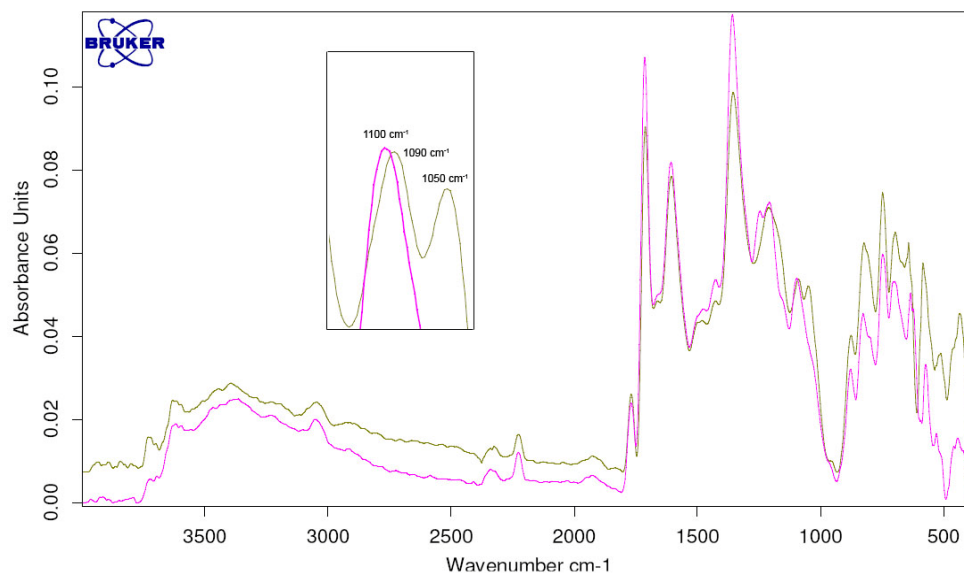
Figure 4.6: IR spectra of both unconditioned (pink) and conditioned (green) CMS membranes. The key, noticeable difference is shown in the inset. The sulfoxide functional group is present at 1050 cm^{-1}.

4.7 Effect of Oxygen Doping on H_2S Conditioned State

Kiyono has already shown the effect that oxygen doping has on CMS transport properties [1,2], so another set of experiments was carried out to further understand the

role oxygen doping may have during H_2S conditioning. The rapid conditioning protocol was carried out on CMS membranes pyrolyzed in an 11 ppm O_2 in Ar atmosphere to determine the similarity of the conditioned steady states depending on the degree of oxygen doping. Figure 4.7 indicates that 11 ppm oxygen doped CMS membranes condition after a similar H_2S exposure time period as 2 ppm oxygen doped CMS membranes. However, the 11 ppm oxygen doped CMS membranes approach a very different conditioned state, suggesting an inverse relationship between amount of oxygen doping and the conditioned state CO_2 permeability of the material. The data is also shown in Table 4.4. The conditioned state of the 11 ppm oxygen doped membranes has ~60% less permeance compared to the unconditioned state. These data also suggest that the H_2S conditioning effectively decreases the size of sieving ultramircopores causing an increase in selectivity as proposed in the previous section.
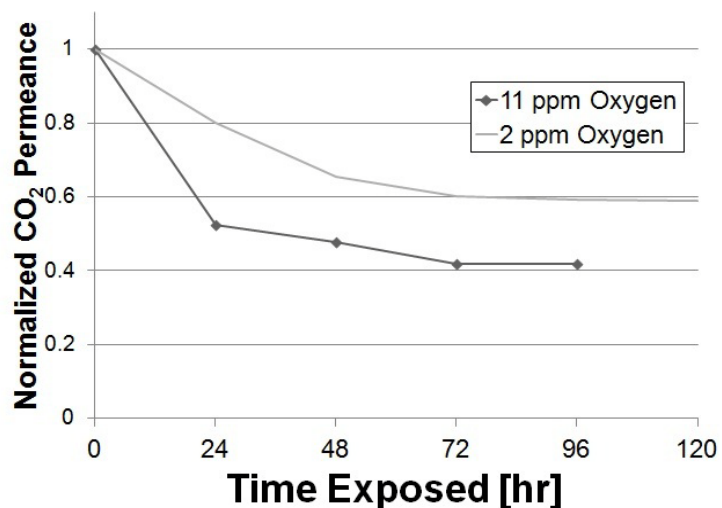
Figure 4.7: Pure gas CO_2 permeation change as a function of time exposed to the rapid conditioning mixed gas feed. CMS hollow fiber membranes produced via pyrolysis at 500 °C with 11 ppm O_2 in Ar pyrolysis atmosphere.

Table 4.4: Permeance and selectivity of CMS membrane after H_2S exposure via the rapid conditioning protocol. CMS membrane prepared pyrolysis at 500 °C with 11 ppm O_2 in Ar pyrolysis atmosphere.

| Total H_2S Exposure [hr]	CO_2 Permeance [GPU]	% Decrease in CO_2 Permeance [--]	CO_2/CH_4 Selectivity [--]	H_2S/CH_4 Selectivity [--]
0	2.1	--	55.8	--
24	1.1	45.3	--	18.3
48	1.0	50.1	--	--
72	0.88	57	79.8	29.7
96	0.88	57	81.2	29.9

The conditioned state of the 11 ppm oxygen doped membrane has a much higher CO_2/CH_4 selectivity compared to the 2 ppm oxygen doped membrane, but the CO_2 permeance is almost an entire order of magnitude smaller. The H_2S/CH_4 selectivity is also twice as high as the 2 ppm doped membrane. These significant differences in transport properties highlight the importance of oxygen doping in CMS membranes. The modeled rate constant for the 11 ppm doped membrane is $1.41 \cdot 10^{-2}$ s^{-1} as opposed to $7.56 \cdot 10^{-3}$ s^{-1} for the 2 ppm doped membrane indicating faster chemisorptions for the higher oxygen doped membranes. The data show that the transport properties of conditioned membranes are "tunable" by controlling the oxygen present just as they are "tunable" in unconditioned membranes [2].

The complete representation of oxygen doped CMS membranes performed in this study is shown in Figure 4.7. The permeance values from the asymmetric hollow fibers used in this study were converted to permeability by assuming a skin thickness of 30 μm. CMS hollow fiber membranes produced from Matrimid® collapse during pyrolysis [18], which justifies the use of a condensed skin layer to calculate the permeabilities.. The porous substructure of the polymer precursor fibers is lost during pyrolysis resulting in a relatively thick fiber in which nearly the entire wall thickness is a dense selective layer. The data presented and results from Xu et al. [18] indicate that

Matrimid® derived CMS fiber membranes have considerably lower permeances despite the high permeability of CMS dense films.
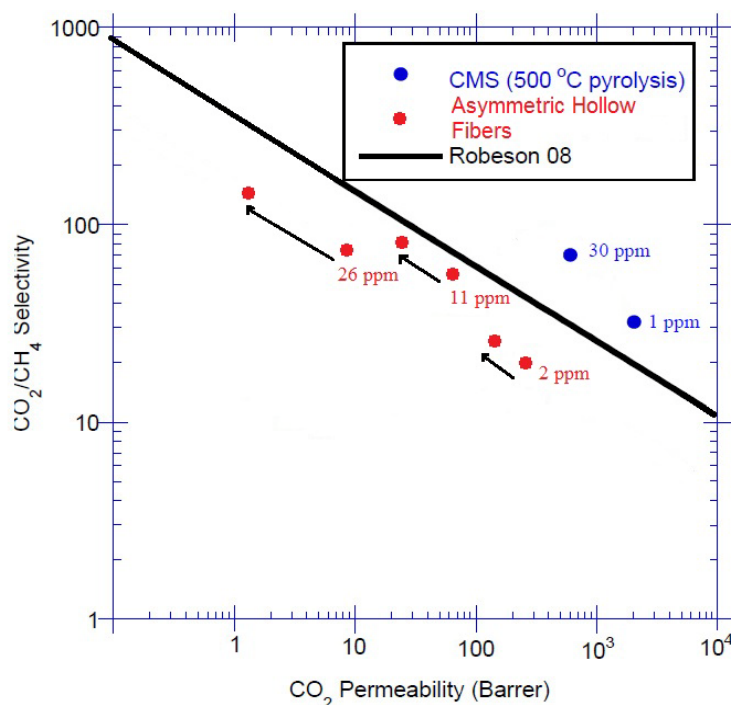
Figure 4.8: Comparison between CMS hollow fibers from this study and dense film work performed by Kiyono [1,2]. The arrows represent the change from the unconditioned to the hypothetical conditioned state.

4.8 Reversibility of H$_2$S Conditioning

Menendez has shown that the conditioning of CMS membranes that takes place due to exposure to a wide variety of atmospheres is not completely reversible [8], though H$_2$S atmospheres were not looked at. It has been shown that with adequate regeneration a fraction of the transport properties lost due to conditioning can be recovered [1,8]. The extent to which the pure gas permeation can be restored via long term (> 30 days) vacuum exposure and long term (> 30 days) storage under positive CO$_2$ pressure (30 psi$_g$) has been tested.

Table 4.5: Permeance and selectivity of CMS membrane after attempted regeneration of transport properties following H_2S. The membranes tested were 2 ppm O_2 in Ar pyrolyzed at 500 °C.

Regeneration Method Used [--]	Unconditioned CO_2 Permeance [GPU]	Unconditioned CO_2/CH_4 Ideal Selectivity [--]	Conditioned CO_2 Permeance [GPU]	Conditioned CO_2/CH_4 Ideal Selectivity [--]	Regenerated CO_2 Permeance [GPU]	Regenerated CO_2/CH_4 Selectivity [--]
Vacuum	8.9	16.4	5.8	25.4	5.0	26.5
CO_2 Atmosphere	10.1	17.6	5.0	26.7	4.9	28.2

The membranes on which the regeneration methods were performed had already been fully H_2S conditioned. The data shown in Table 4.5 indicates that over the course of the regeneration study the transport properties were unable to be even partially recovered as has been reported to be possible when CMS membranes are conditioned by H_2O exposure [1,8]. Continued storage in vacuum allowed the membrane to further condition as the permeance decreased by ~14% while the selectivity increased by ~1%. The storage of CMS membranes under CO_2 however offers a more promising result. The module that was regenerated by continuous exposure to CO_2 showed no continued conditioning, though it also showed no recovery of transport properties.

Although the transport property changes due to H_2S conditioning were unable to be regenerated with either of the two regeneration protocols, the CO_2 storage results are encouraging from an industrial prospective. It is known that water vapor from the atmosphere has a very negative impact on the transport properties of CMS membranes [1,2]. An industrial supplier of CMS membrane modules would have to deliver its modules to its customers while avoiding humidity exposure. The option to store the modules under CO_2 is a much more economical option compared to vacuum storage. Additionally, if the modules are to be H_2S conditioned before being supplied to a customer, the results above would indicate that vacuum storage would be less than ideal for a conditioned membrane.

4.9 References

[1] Kiyono M. Carbon molecular sieve membranes for natural gas separations. Atlanta GA USA, Georgia Institute of Technology, 2010.

[2] Kiyono M, Williams PJ, Koros WJ. Effect of pyrolysis atmosphere on separation performance of carbon molecular sieve membranes. J Membr Sci 2010; 359(1-2):2-10.

[3] Vu DQ, Koros WJ, Miller SJ. Mixed matrix membranes using carbon molecular sieves-I. Preparation and experimental results. J Membr Sci 2003; 211(2):311-334.

[4] Vu DQ, Koros WJ, Miller SJ. Mixed matrix membranes using carbon molecular sieves-II. Modeling permeation behavior. J Membr Sci 2003; 211(2):335-348.

[5] Kiyono M, Williams PJ, Koros WJ. Effect of polymer precursors on carbon molecular sieve structure and separation performance properties. Carbon 2010; 48(15):4432-4441.

[6] Pesek SC, Koros WJ. Aqueous quenched asymmetric polysulfone membranes prepared by dry/wet phase separation. J Membr Sci 1993; 81:71-88.

[7] Pesek SC, Koros WJ. Aqueous quenched asymmetric polysulfone hollow fibers prepared by dry/wet phase separation. J Membr Sci 1994; 1994:1-19.

[8] Menendez I, Fuertes AB. Aging of carbon membranes under different environment. Carbon 2000; 39:733-40

[9] Carruthers SB, Ramos GL, Koros WJ. Morphology of integral-skin layers in hollow fiber gas separation membranes. J Appl Polym Sci 2003; 90:399-411.

[10] McKelvey SA, Clausi DT, Koros WJ. A guide to establishing hollow fiber macroscopic properties for membrane applications. J Membr Sci 1997; 124:223-32.

[11] Vu DQ, Koros WJ, Miller SJ. High pressure CO_2/CH_4 separation using carbon molecular sieve hollow fiber membranes. Ind Eng Chem Res 2002; 41(3):

[12] Xu LR, Rungta M, Koros WJ. Matrimid (R) derived carbon molecular sieve hollow fiber membranes for ethylene/ethane separation. J Membr Sci 2011; 380(1-2):138-147.

[13] Wallace DW. Crosslinked hollow fiber membranes for natural gas purification and their manufacture from novel polymers. Austin TX USA, University of Texas at Austin, 2004.

[14] Kosuri MR, Koros WJ. Defect-free asymmetric hollow fiber membranes from Torlon (R), a polyimide-imide polymer, for high-pressure CO_2 separations. J Membr Sci 2008; 320(1-2):65-72.

[15] Pye DG, Hoehn HH, Panar M. Measurement of gas permeability of polymers. 1. Permeabilities in constant volume/variable pressure apparatus. J Appl Polym Sci 1976; 20(7):1921-31

[16] Pye DG, Hoehn HH, Panar M. Measurement of gas permeability of polymers. 2. Apparatus for the determination of permeabilities of mixed gases and vapors. J Appl Polym Sci 1976; 20(2):287-301

[17] Chen CC. Thermally crosslinked polyimide hollow fiber membranes for natural gas purification. Atlanta GA USA, Georgia Insititute of Technology, 2011.

[18] Xu LR, Rungta M, Koros WJ. Matrimid (R) derived carbon molecular sieve hollow fiber membranes for ethylene/ethane separation. J Membr Sci 2011; 380(1-2):138-147.

[19] Papirer E, Li S, Vidal A. Formation of carbon black-sulfur surface derivatives by reaction with P_2S_5. Carbon 1991; 29(7):963-968.

[20] IglamovaNA, Mazitova FN, Shagidullin RR, Doroshkina GM, Ivanov VG, Kabatskaya IS. Determination of sulfoxides and sulfones by IR spectroscopy. Chem & Tech of Fuels and Oils 1990; 26(9-10):557-558.

CHAPTER 5

SUMMARY AND RECOMMENDATIONS

5.1 Summary and Conclusions

The goal of this project was to identify the steady state transport properties of CMS membranes upon conditioning via long term exposure to high H_2S chemical activity. To identify the conditioned state an industrially relevant, aggressive extended conditioning protocol was used to condition the membranes. In order to determine if the conditioning was a function of H_2S chemical activity exposure, a second, rapid conditioning protocol was explored. It was important to determine if the states reached through the different conditioning protocols led to the same steady state transport properties as the rapid conditioning protocol would be industrially favored for membrane module production. A hypothesis was proposed that the conditioned steady state would be reached after a set exposure time to a constant H_2S chemical activity.

The results from Matrimid® based CMS membranes pyrolyzed in a 2 ppm O_2 in Ar atmosphere indicate that the same steady state is reached after both of the conditioning protocols are followed. This indicates that the final conditioned steady state is not likely path dependent and is a function of time exposed to H_2S. There is a difference between the amount of time it takes to reach the conditioned state between the two different conditioning protocols; however, the ultimate end point appears to be a function of the H_2S level (and presumably temperature) as it is for oxygen doping at high temperatures. The first rate reaction model indicates that the reaction rate constants are different between each of the conditioning protocols. The extended conditioning protocol contains two additional gases which most likely decrease the available sorption sites for H_2S. Carbon dioxide is a highly sorbing gas that is present in equal mol % in the high

pressure mixed gas feed. The presence of CO_2 clearly increases the time it takes for H_2S conditioning to occur.

Once it was determined that the rapid conditioning protocol led to a steady state conditioned state the rapid conditioning protocol was carried out on CMS membranes that had different oxygen doping to probe the effect oxygen doping has on H_2S conditioning. The results show that the time required to reach the conditioned state is nearly the same regardless of oxygen doping. However, the conditioned state reached is highly dependent on oxygen doping. For the 11 ppm O_2 doped membrane the conditioned state exhibited approximately ~40% of the unconditioned membrane permeance, and for the 26 ppm O_2 doped membrane the conditioned state exhibited approximately ~17% of the unconditioned membranes permeance. In all cases the CO_2/CH_4 selectivity increased with the corresponding decrease in pure gas permeances. The H_2S conditioning clearly has a larger effect on CH4 permeance than it has on CO_2 permeance.

Finally, the H_2S conditioning was shown to not be reversible by typical CMS regeneration methods [1]. Both the long term storage of the CMS membranes under vacuum and in a CO_2 atmosphere did not regenerate the membranes. Typically vacuum and elevated temperature is enough to remove non-condensable gases and unreactive atmosphere exposure can cause swelling which can recover some of the permeance lost during H_2S conditioning [1,2]. This was not observed using the regeneration methods described in this work.

5.2 H_2S Conditioning of Non-collapsed CMS fibers

Recent advances in preventing the porous substructure collapse during pyrolysis have produced CMS fiber membranes that do not suffer the high separation layer thickness exhibited by collapsed CMS fibers used in this work. These proprietary fibers were provided by Nitesh Bhuwania in the Koros Group. By decreasing the separation

layer thickness the CMS fibers may lie above the Robeson upper bound due to the high permeability seen in CMS dense films. Preliminary data show these fibers can exhibit a wide range of transport properties depending upon the pyrolysis temperature. One pyrolysis temperature led to fibers with a CO_2 permeation of 112 GPU with a CO_2/CH_4 selectivity of 15. A second pyrolysis temperature led to fibers with a CO_2 permeation of 19 GPU with a CO_2/CH_4 selectivity of 96 and an H_2S/CH_4 selectivity of 20 when H_2S was measured at 30 psia. Preliminary work using these non-collapsed fibers shows that these fibers also exhibit an H_2S conditioning effect upon exposure to H_2S, as expected. However, the highly aggressive H_2S conditioning used in this study should be avoided as the conditioned state in these fibers exhibited a permeance less than 1% of the unconditioned fibers and a selectivity decrease. The data for the conditioned state for these non-collapsed fibers show the size discriminating ultramicropores to be effectively shut down, resulting in the significant drop in permeance. The kinetic rate constant for these non-collapsed fibers is also much higher than the collapsed CMS fibers used in this study as these CMS fibers reach the conditioned state in less than 48 hours. Future work should involve understanding this change in transport properties as the effective shut down of the discriminating micropores was an unexpected result.

5.3 Extensive Sorption Studies

The solubility of H_2S in CMS under various conditions is very important in understanding the fundamental transport of H_2S in CMS membranes. Gas sorption experiments should be carried out to characterize sorption coefficients, hole filting capacity, and the affinity constant of CO_2, H_2S, and CH_4 in both conditioned and unconditioned CMS membranes [4]. Ideally, performing CO_2 and CH_4 sorption after consecutive conditioning soaks would allow one to probe the effect H2S conditioning has on the available sorption sites during permeation. The difference in H_2S sorption

between a conditioned and unconditioned membrane should also allow the refinement of the H_2S conditioning model described in Chapter 4.

Determining sorption coefficients, hole filling capacity, and the affinity constant for a wide range of gas molecules, including both condensable and non-condensable gases, on conditioned and unconditioned CMS membranes could allow better determination of the entropic and energetic contributions to H_2S permeability and the changes undergone during and after H_2S conditioning. These sorption studies combined with the permeability data would allow the accurate calculation of diffusivity coefficients. Knowing the effect H_2S conditioning has on both solubility and diffusivity coefficients will help us better understand the way H_2S chemisorptions is taking place. These results would also allow one to check the proposed representation of H_2S chemisorptions at both the ultramicropore and micropore sites as outlined in Figure 4.4.

5.4 Alternative Regeneration Method

The regeneration methods described in Section 4 represent common regeneration techniques [1]. The results show that H_2S conditioned CMS membranes do not readily recover transport properties after these regeneration methods are used. Another common regeneration method would be to expose the conditioned CMS membranes to propylene. Propylene causes the CMS membrane to swell and also flushes out sorbed gases, notably water vapor [1,3]. Jones and Koros have shown that propylene acts as a cleansing agent and removes a wide variety of organic contaminants.

5.5 References

[1] Menendez I, Fuertes AB. Aging of carbon membranes under different environment. Carbon 2000; 39:733-40.

[2] Kiyono M. Carbon molecular sieve membranes for natural gas separations. Atlanta GA USA, Georgia Institute of Technology, 2010.

[3] Jones CW, Koros WJ. Carbon molecular sieve gas separation membranes-II. Regeneration following organic exposure. Carbon 1994; 32(8):1427-32.

[4] Kiyono M, Williams PJ, Koros WJ. Effect of polymer precursors on carbon molecular sieve structure and separation performance properties. Carbon 2010; 48(15):4432-4441.